Title
Ce Cation Migration and Diffusivity in Perfluorosulfonic Acid Fuel Cell Membranes

Journal
ECS Transactions, 92(8)

ISSN
1938-5862

ISBN
9781607688822

Authors
Baker, Andrew M
Babu, Siddharth Komini
Chintam, Kavitha
et al.

Publication Date
2019-07-03

DOI
10.1149/09208.0429ecst

Ce Cation Migration and Diffusivity in Perfluorosulfonic Acid Fuel Cell Membranes

A. M. Baker[a], S. K. Babu[a], K. Chintam[a], A. Kusoglu[b], R. Mukundan[a], and R. L. Borup[a]

[a] Los Alamos National Laboratory, Los Alamos, NM 87545, USA
[b] Lawrence Berkeley National Laboratory, Berkeley, CA 94720, USA

An H_2 pump experiment was utilized to simultaneously determine the migration and diffusivity of Ce ions in perfluorosulfonic acid ionomer membranes over a range of temperatures and relative humidities. Ce ion migration profiles were quantified as a function of charge transfer through the cell using X-ray fluorescence (XRF). Competing transport phenomena were decoupled by fitting XRF profile data with our previously-developed one-dimensional model, which was updated with improved conductivity and water uptake relations. Measured transport values showed good agreement with the Einstein relation and with Okada transport theory, additionally implying that conductivity measurements can be used to estimate migration and diffusivity of cations in other cation/PFSA systems. Results presented here may be used to populate device-level models in order to further understand the effects of cation transport on fuel cell performance and durability to determine the mitigation controls for Ce stabilization.

Introduction

Cerium enhances the durability of perfluorosulfonic acid (PFSA) ionomer-based polymer electrolyte membrane (PEM) fuel cells by scavenging reactive radical species which are generated during operation (1). However, we have shown that during cell fabrication, conditioning, and operation, Ce dissolves and is transported within the membrane electrode assembly (MEA) due to gradients in ionomer hydration [convection (2,3)], ionomer potential [migration (4–6)], and cationic concentration [diffusion (4,7)]. Ce transport is detrimental because (i) its accumulation in the CL ionomer can disrupt proton and/or oxygen transport to the catalyst, which results in sub-optimal performance, especially at high current density (8,9); and (ii) its depletion may leave an ionomer region more susceptible to radical attack. Therefore, it is of interest to quantify these transport mechanisms under a range of operating conditions in order to understand their effects on cell performance/durability and determine the necessity for further Ce stabilization, either through materials development or system control strategies.

Experimental

Determination of Diffusivity and Migration

To determine in-plane Ce ion migration and diffusivity at different relative humidity (RH) and temperature (T) conditions, H_2 pump experiments were performed in a standard conductivity cell (Scribner Associates, Inc.). Nafion™ NR-211 PFSA PEMs (Ion Power,

Inc.) were doped to ~5% Ce exchange in-house using Ce(III) nitrate according to the method of Greszler and coworkers (10).

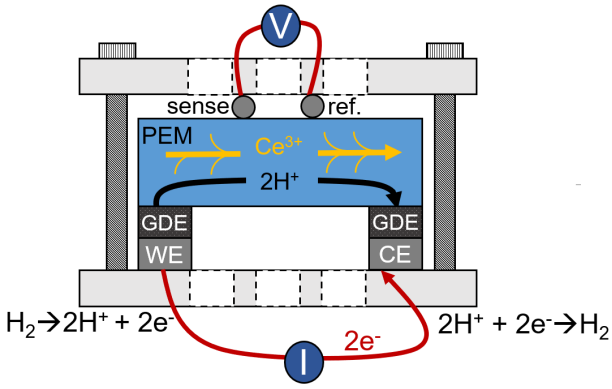

Figure 1. A schematic cross-sectional view of the H_2 pump experiment performed in a T and RH-controlled conductivity cell.

The conductivity cell was assembled using standard procedures (10) as shown in Figure 1. In simultaneous migration/diffusion experiments, the hydrogen oxidization reaction (HOR) and hydrogen evolution reaction (HER) are catalyzed either end of the specimen using gas diffusion electrodes (GDEs) placed between the specimen and the Pt mesh working (WE) and counter (CE) electrodes, respectively. 2 mg_{Pt} cm^{-2} carbon paper-based GDEs (Fuel Cells, Etc.) were hot pressed to the membrane at 140°C with ~10 MPa of pressure for 10 minutes prior to specimen installation. In diffusion-only experiments, where no potential gradient-driven Ce migration was induced, no GDEs were used.

After specimen installation, the cell was installed in standard 25 cm^2 single-cell fuel cell hardware (Fuel Cell Technologies), with graphite bipolar plates and polyurethane gaskets. The assembled cell was connected to a fuel cell test stand (Fuel Cell Technologies) which was used to maintain constant cell temperature, as well as gas RH and flow rate, throughout the duration of each experiment. Cells were operated at temperatures between 23 and 80°C in H_2 at RHs between 25 and 100% with an H_2 flow rate of 0.2 standard liters per minute (SLPM) in order to provide an excess of H_2 to the system. Outlet pressures were maintained at 101 kPa_{abs} using the test stand. Prior to testing, specimens were equilibrated under the prescribed T/RH condition for 1 hour.

A potentiostat (BioLogic SP-50) with EC-LAB control/data acquisition software was used to maintain a constant potential gradient of 0.25 V between the sense and reference electrodes. This resulted in a nominal potential gradient of 0.75 V in the membrane between the WE and CE, which is expected to keep Ce ions in the reduced trivalent state at all pH < 4 (11). After every 0.25 to 0.5 Coulombs (C = I * t) of charge transfer, the potentiostat was turned off, the leads were disconnected, if used, the cell was dried, and intermittent Ce profiles were measured. The transport model described below was used to simultaneously fit the migration and diffusivity values.

Ex Situ Diffusion Experiments. In order to isolate the effects of diffusion in the absence of migration, *ex situ* "salt dip" experiments were performed, similar to the "dot

doping" method utilized by Coms and McQuarters (7). A 5 x 25 mm, Ce-free membrane specimen was folded in half, supported by a macroporous PTFE mesh, and partially submerged for 10 minutes into a 10 mM Ce(III) nitrate solution which was agitated with a stir bar. The specimen was removed from the solution, rinsed with deionized water, and dried in air for 1 hour. The resulting Ce profile was measured using XRF and taken as the initial profile before diffusion. The specimen was installed in the conductivity cell, as described above and exposed to 100% RH H_2 at 80°C without any applied potential gradient. Intermittent XRF profiles were taken every 2 hours, and the transport model was fit to the data using a single diffusivity value.

Serial Migration and Diffusion. Like our previous work, diffusivity values were also obtained by initially migrating a large Ce gradient in the membrane under the CE and then letting it diffuse in the absence of a potential gradient (4). This was done with a GDE-free membrane specimen with uniform ~5% Ce exchange. After the initial migration, the Ce profile was measured using XRF. The specimen was re-installed in the conductivity cell, as described above and exposed to humidified H_2 at 80°C and 100% RH without any applied potential gradient. Intermittent XRF profiles were taken every 2 hours, and the diffusivity value, alone, was fit using the transport model.

X-ray Fluorescence Analysis of Ce Profiles

In order to measure intermittent Ce distributions, PEM specimen were dried in the cell hardware at the corresponding temperature with dry N_2 for 5 minutes before removal from the conductivity cell hardware. As shown in our previous work, at low RHs, diffusion effects are negligible for durations below 2 hours, thus, the Ce profiles measured in the PEM after drying are assumed to be representative of those after the corresponding transport processes (convection, migration, and/or diffusion).

Ce area density fluorescence profiles, in counts cm^{-2}, were measured in air using a micro-XRF analyzer (EDAX Orbis) with a spot size of 30 μm, a 35 μm thick nickel filter, an accelerating voltage of 30 kV, and a tube current of 700 μA. 256 point line scans were performed along the midline of the PEM, with a duration of 4 sec $point^{-1}$. All XRF analysis was based on the relative intensity of fluoresced Ce L-lines, which are the most prominent fluorescent X- rays emitted by Ce and arise at energy levels of 4.84 keV. Ce area density measurements from XRF were normalized to the initial ionomer Ce exchange fraction of ~5%.

Transport Model

XRF profiles were fit using an updated version of our previously-developed transient, 1-D transport model in order to decouple the competing transport effects (4). The model was modified to capture changes in (i) conductivity and (ii) λ (defined as nH_2O/SO_3^-) due to local Ce ion exchange and to (iii) simplify determination of the PEM potential gradient by utilizing a 4-electrode control mode, instead of the 2-electrode mode used in our previous work.

Changes in Ce concentration (c_{Ce}) with time (t) were modeled using the 1-D Nernst-Planck equation in the form of:

$$\partial c_{Ce} / \partial t = \nabla . [(D_o * f(c_{Ce}, RH) * \nabla c_{Ce}) + (u_m * c_{Ce} * \nabla \phi_{ionic})] \quad [1]$$

where D_o the prefactor related to Fickian diffusivity and $f(c_{Ce}, RH)$ is the local hydration, λ, calculated as a function of Ce sulfonic acid site exchange fraction (f_{Ce}, where f_{Ce} =1 is full Ce exchange) and RH (similar to Equation 2). This approach improved the quality of fit compared to using a constant diffusivity value, alone. Herein, all diffusivity values are reported as D_{avg}, which is calculated as the product of D_o and the average λ in the sample over the course of the experiment. Since local hydration only changes slightly with increased Ce content, the deviation of these values was typically less than 5% of the average, as will be shown. This effect could be much larger when considering cation doped PFSA systems with large λ variations, such as monovalent cations, like Ca^+ and K^+ (14). In this work, D_{avg} values were in the same order of magnitude as diffusivities measured in similar experiments (7). λ was determined as a function of RH and f_{Ce}, as will be shown in an upcoming work (12). At 100% RH, λ is expressed as:

$$\lambda = 10.5 - 2.1 * f_{Ce} \quad [2]$$

It should be noted that these values were measured at 25°C but are not expected to change significantly with increasing temperature (13). u_m is the migration coefficient and ϕ_{ionic} is the ionic potential.

Identical to our previous work, HOR/HER is represented using the Butler-Volmer Equation (Reference 4, Equations 3 and 4). Ionic and electronic charge conservation are applied to the model domain and electrodes, respectively, (Reference 4, Equations 5 and 6, respectively), however the ionic conductivity (σ_{ionic}), in mS cm^{-1}, was updated as a function of T, RH and f_{Ce} as will also be shown in an upcoming work (12). At 80°C and 100% RH, σ_{ionic} is expressed as:

$$\sigma_{ionic} = 10.5 * \exp(100 * f_{Ce} - 0.02) \quad [3]$$

Furthermore, utilization of the 4-electrode mode allowed for direct determination of the electrical potential gradient in the membrane, thus eliminating the need to calculate the potential in the working electrode. The CE is defined as the reference, with an electric potential equal to zero.

Charge and mass conservation were modeled using a transient solver with a time step of one second in COMSOL Multiphysics v5.3 with no flux boundary conditions similar to our previous work (Reference 4, Equations 7 and 8). For each experiment and condition, the appropriate coefficients were fit using the least squares method in order to minimize the sum of the squared residuals among all corresponding XRF profiles.

Results and Discussion

Simultaneous Determination of Ion Migration and Diffusion Coefficients

Validation of H_2 Pump Technique. In order to validate the H_2 pumping method as an internally consistent technique to quantify both cation migration and diffusivity simultaneously, two separate methods of determining diffusion coefficients were

employed. As shown in Figure 2a, the "salt dip" method was used to introduce Ce into a PFSA specimen *ex situ* (0 hour profile). The specimen was installed in the conductivity cell and exposed at 80°C and 100% RH H_2, without any applied potential. A single diffusivity parameter was used to fit the intermittent Ce profiles with the transport model, where the migration and convection coefficients were assumed to be zero. Fitting results in a D_{avg} value of 9.5 x 10^{-7} cm^2 s^{-1}.

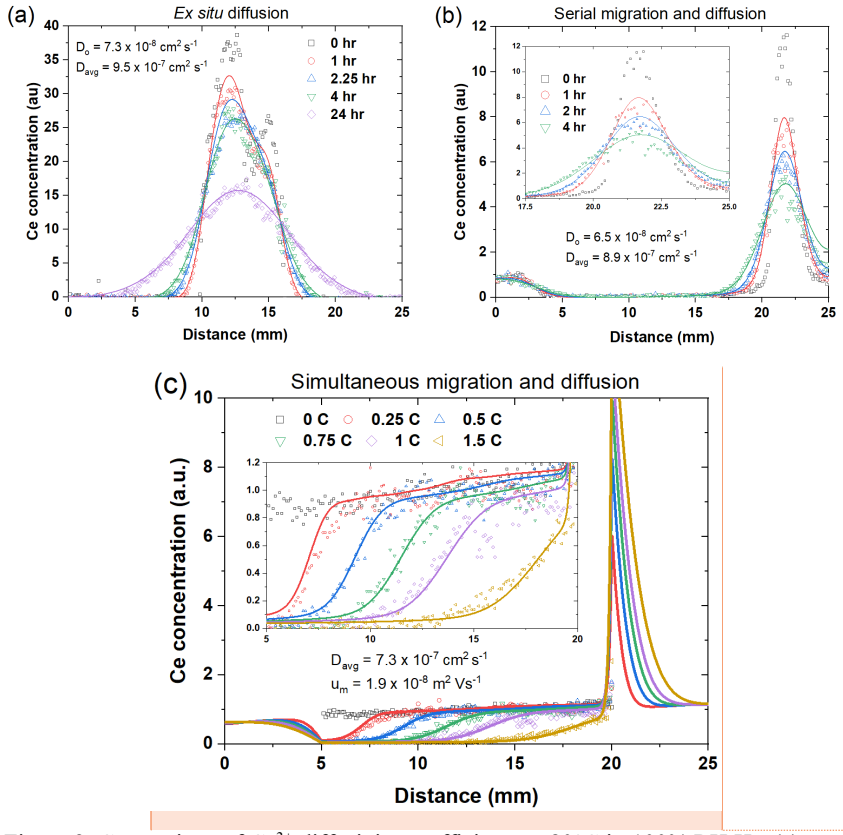

Figure 2. Comparison of Ce^{3+} diffusivity coefficients at 80°C in 100% RH H_2: (a) *ex situ* salt dip experiments, (b) serial migration and diffusion experiments, and (c) simultaneous fitting of H_2 pump diffusion/migration experiments. Ce profiles measured using XRF are shown by the symbols, while the solid lines represent the transport model fits.

In a similar vein to our previous work, Ce diffusivity was also assessed by serially inducing a concentration gradient by migration into the CE of the conductivity cell and then letting it diffuse in the conductivity cell under identical conditions to the salt dip experiment, as shown in Figure 2b. Fitting results yielded a D_{avg} value of of 8.9 x 10^{-7} cm^2 s^{-1}; which was about 6% of the previous value.

Figure 2c shows the results of the H_2 pump experiment also performed at 80°C in 100% RH H_2, where Ce migration is induced by the potential gradient between the WE

Commented [AB1]: Add electrode data

and CE. Here, the transport model was used to simultaneously fit the 5 intermittent profiles with 2 parameters (migration and diffusion coefficients). Here, a D_{avg} value of 7.28 x 10^{-7} cm^2 s^{-1} was obtained. The D_{avg} value obtained by simultaneous fitting was in in excellent agreement with the values from the other two techniques. This result implies that a single H_2 pump experiment can be used to quantify migration and diffusivity.

Ce Cation Migration and Diffusivity

Using the H_2 pump experiment described above, diffusivity and migration coefficients were determined under a range of temperatures (23-80°C) and humidification conditions (25-100% RH). D_{avg} and u_m are reported as functions of λ_{avg}, where D_{avg} and λ_{avg} are the average local diffusivity and hydration in the membrane during the experiment. The results in Figure 3a show a monotonic increase of diffusivity with hydration level and temperature. The results obtained here are generally in the same order of magnitude as the diffusivity values obtained by Coms and McQuarters (7), the specific values here are lower, especially at higher RHs. The difference could be attributed to our use of the Nernst-Planck model instead of the steady-state solution in their work. Diffusivity of Ce in liquid water was also measured to be 0.2 to 2 x10^{-8} cm^2 s^{-1} by Zaton et al. using ion chromotography (15), which is lower than the results obtained here (0.88 x 10^{-6} cm^2 s^{-1}) and by Coms and McQuarters (2.0 x 10^{-6} cm^2 s^{-1}) under similar conditions.

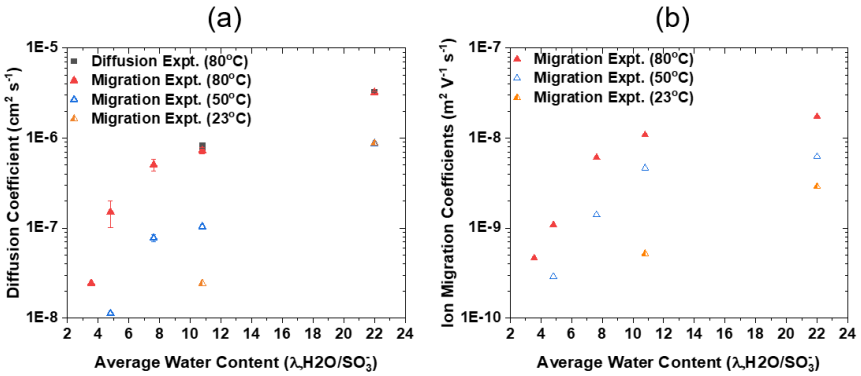

Figure 3. (a) Diffusivity (D_{avg}) and (b) migration coefficients of Ce^{3+} in Nafion™ NR-211 PFSA membranes determined using H_2 pump migration experiments over a range of temperatures and hydration levels. Diffusion-only experiments in the absence of potential gradients are also shown in (a).

Figure 3b shows that the ion migration follows similar monotonic effects with hydration and temperature, like diffusivity. Assuming both the diffusivity and migration are equal to zero at $\lambda = 2.3$, fitting data in the water vapor regime (λ = 2.3-14) at 80°C yields power law relations in the form of:

$$D = 1.06 \times 10^{-8} * \lambda^{1.80} \quad (R^2 = 0.920) \qquad [4]$$

$$u_m = 6.32 \times 10^{-11} * \lambda^{2.18} \quad (R^2 = 0.961) \qquad [5]$$

Similar relationships can be obtained at 50 and 23°C. These relationships, in conjunction with Equations 2 and 3, may be used to directly inform models to solve for Ce cation convection. Once all three transport mechanisms are determined, device-level models can quantify the effect of operating conditions on 3-D cation movement and its subsequent effects on sulfonic acid group solvation and ionomer conductivity.

Validation of the Einstein Relation. While it is possible that ion migration behavior through hydrated poly(anion) electrolytes with nano- and mesoscale ordering, such as PFSAs, may not strictly follow the migration of free cations in solution (16), using this expanded data set, we revisited the Einstein relationship, in an attempt to simplify the transport analysis. In our previous work, we showed the improved accuracy of model fits compared to migration coefficients determined by the Einstein relation ($u_{m,E}$) of the form:

$$u_{m,E} = (z * D * F) / (R * T) \quad [6]$$

where z is the cation valance, F is the Faraday constant, D is the experimentally-determined diffusivity (here, D_{avg}), R is the ideal gas constant, and T is the temperature, in Kelvin.

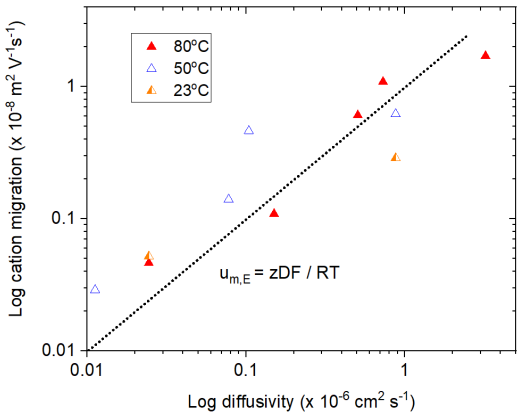

Figure 4. Cation migration as a function of diffusivity across a range of temperatures and RHs obtained using the H_2 pump technique. The solid line represents a linear fit of the migration values calculated using only the Einstein relation (Equation 6) and the diffusion coefficients determined from H_2 pump experiments.

Figure 4 shows a plot of experimentally-determined migration coefficients vs. measured diffusivity values (D_{avg}). The overlaid line represents migration values calculated from the Einstein relation (Equation 4) using only these diffusivities. All independently-determined migration values fell reasonably close to the results calculated using this relation. In addition, there is no apparent trend in deviation of experimental migration coefficients from the Einstein relation across the Ts and RHs tested. These results imply that the Einstein relation may be employed to elucidate migration from simple diffusion experiments with reasonable accuracy.

Comparison of Results to Okada Theory. To further simplify transport analysis, Okada transport theory, which derives cation migration from membrane conductivity (17), was

also revisited using this expanded dataset. From Okada's analysis (Reference 17, Equation 11), conductivity-derived ion migration coefficients ($u_{m,\kappa}^{o}$) were calculated as:

$$u_{m,\kappa}^{o} = \kappa^{o} / F * c_{SO3-} \quad [7]$$

where κ^{o} is the conductivity of fully-exchanged PEMs, in S m^{-1} and c_{SO3-} is the concentration of sulfonic acid groups ($c_{SO3-} = \rho / EW$), here equal to 1.8 x 10^{3} mol m^{-3} (17). This value may be taken as constant, assuming that migration does not change as a function of cation doping level (17).

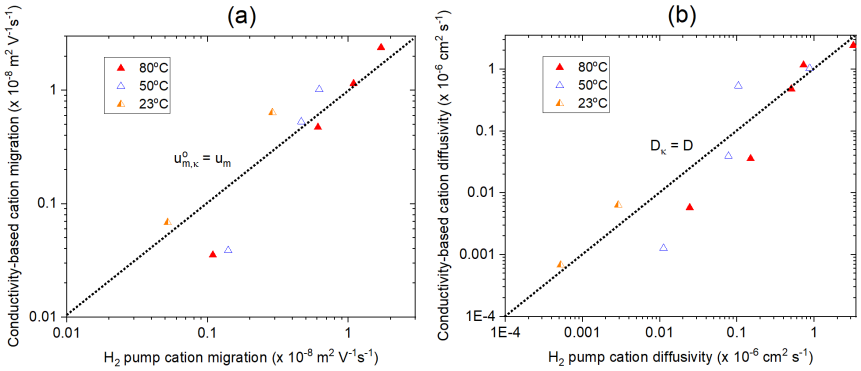

Figure 5. Conductivity-based (a) migration and (b) diffusivity values plotted as a function of values obtained via H_2 pump experiments over a range of Ts and RHs. D_κ values shown in (b) were obtained using $u_{m,\kappa}^{o}$ with the Einstein relation (Equation 6). The dotted line shows unity where either calculated migration or diffusivity is equal to experimentally-determined values.

$u_{m,\kappa}^{o}$ was calculated for every T/RH condition corresponding to the H_2 pump experiments using the conductivity of saturated membranes, as will be shown in our upcoming work (12). The reciprocal of Equation 6 was used to calculate diffusivity (D_κ) from the calculated $u_{m,\kappa}^{o}$ values. Figure 5a and b show the calculated $u_{m,\kappa}^{o}$ and D_κ values plotted against the u_m and D_{avg} values, respectively, determined from the H_2 pump experiments. The lines shown in both plots represent unity where calculated and experimental coefficients are equal. The conductivity-derived transport coefficients were in good agreement with our experimental data across the range of Ts and RHs tested. Thus, measuring conductivity of a fully exchanged PEM at a given T/RH condition can be used in conjunction with the approach described here in order to give a reasonable approximation of migration and diffusivity at that condition with a single experiment.

Conclusions

In this work, we showed that diffusivity values obtained by simultaneous diffusivity/migration fitting of our H_2 pump experiments were internally consistent with *ex situ* diffusion experiments. Experiments were performed over a range of Ts and RHs to develop empirical relationships between transport and temperature/hydration. These

results are useful to directly inform Ce transport in convection experiments and device-level models with high accuracy.

A simple approach to quantify cation transport was also investigated. The expanded dataset was used to validate the Einstein relation and Okada analysis, which suggests that accurate diffusion and migration coefficients can be obtained with a single conductivity measurement on a fully cation-exchanged PFSA film. Using this approach, migration and diffusivity may be easily estimated over a range of Ts/RHs for the myriad combinations of relevant cations (such as Co, Ni, and Fe) and PFSAs (i.e. varying EW and/or side chain chemistry).

Acknowledgements

This research is supported by the U.S. Department of Energy Fuel Cell Technologies Office, through the Fuel Cell Performance and Durability (FC-PAD) Consortium (Fuel Cells Program Manager: Dimitrios Papageorgopoulos and Technical Development Manager: Greg Kleen).

References

1. F. D. Coms, H. Liu and J. E. Owejan, *ECS Trans.*, **16**, 1735–1747 (2008).
2. A. M. Baker, R. Mukundan, D. Spernjak, E. J. Judge, S. G. Advani, A. K. Prasad and R. L. Borup, *J. Electrochem. Soc.*, **163**, F1023–F1031 (2016).
3. Y.-H. Lai, K. M. Rahmoeller, J. H. Hurst, R. S. Kukreja, M. Atwan, A. J. Maslyn and C. S. Gittleman, *J. Electrochem. Soc.*, **165**, F3217–F3229 (2018).
4. A. M. Baker, S. K. Babu, R. Mukundan, S. G. Advani, A. K. Prasad, D. Spernjak and R. L. Borup, *J. Electrochem. Soc.*, **164**, 1272–1278 (2017).
5. A. M. Baker, D. Torraco, E. J. Judge, D. Spernjak, R. Mukundan, R. L. Borup, S. G. Advani and A. K. Prasad, *ECS Trans.*, **69**, 1009–1015 (2015).
6. Y. Cai, J. M. Ziegelbauer, A. M. Baker, W. Gu, R. S. Kukreja, A. Kongkanand, M. F. Mathias, R. Mukundan and R. L. Borup, *J. Electrochem. Soc.*, **165**, F3132–F3138 (2018).
7. F. D. Coms and A. B. McQuarters, *ECS Trans.*, **86**, 395–405 (2018).
8. D. Banham, S. Y. Ye, T. Cheng, S. Knights, S. M. Stewart, M. Wilson and F. Garzon, *J. Electrochem. Soc.*, **161**, F1075–F1080 (2014).
9. E. L. Redmond, S. M. Wriston and J. L. Szarka III, *ECS Trans.*, **80**, 633–641 (2017).
10. U.S. DOE, *Procedures For Performing In-Plane Membrane Conductivity Testing*, (2008).
11. S. A. Hayes, P. Yu, T. J. O'Keefe, M. J. O'Keefe and J. O. Stoffer, *J. Electrochem. Soc.*, **149**, C623–C630 (2002).
12. K. Chintam, A. M. Baker, A. R. Crothers, X. Luo, R. L. Borup and A. Kusoglu, "Effects of Multivalent Cation Doping on Structure-Functionality of Perfluorosulfonic Acid Membranes and its Fuel Cell Performance," *Manuscript in Preparation.* (2019).
13. A. Kusoglu and A. Z. Weber, *Chem. Rev.*, **117**, 987–1104 (2017).
14. S. Shi, A. Z. Weber and A. Kusoglu, *Electrochim. Acta*, **220**, 517–528 (2016).
15. M. Zatoń, B. Prélot, N. Donzel, J. Rozière and D. J. Jones, *J. Electrochem. Soc.*, **165**, F3281–F3289 (2018).

16. G. Pourcelly, P. Sistat, A. Chapotot, V. Nikonenko and C. Gavach, *J. Memb. Sci.*, **110**, 69–78 (1996).
17. T. Okada, *J. Electrochem. Soc.*, **144**, 2744–2750 (1997).